INVITED PAPER *Special Section on Emerging Communication Technologies in Conjunction with Main Topics of ICETC 2022*

Antennas Measurement for Millimeter Wave 5G Wireless Applications Using Radio Over Fiber Technologies

Satoru KUROKAWA[†a)], **Michitaka AMEYA**[†], **Yui OTAGAKI**[††], **Hiroshi MURATA**[††], ***Members***,
Masatoshi ONIZAWA[†††], **Masahiro SATO**[†††], ***and*** **Masanobu HIROSE**[††††], ***Nonmembers***

SUMMARY We have developed an all-optical fiber link antenna measurement system for a millimeter wave 5th generation mobile communication frequency band around 28 GHz. Our developed system consists of an optical fiber link an electrical signal transmission system, an antenna-coupled-electrode electric-field (EO) sensor system for 28 GHz-band as an electrical signal receiving system, and a 6-axis vertically articulated robot with an arm length of 1 m. Our developed optical fiber link electrical signal transmission system can transmit the electrical signal of more than 40 GHz with more than −30 dBm output level. Our developed EO sensor can receive the electrical signal from 27 GHz to 30 GHz. In addition, we have estimated a far field antenna factor of the EO sensor system for the 28 GHz-band using an amplitude center modified antenna factor estimation equation. The estimated far field antenna factor of the sensor system is 83.2 dB/m at 28 GHz.

key words: *electric field sensor, 5th generation mobile communication, 28 GHz band, antenna measurement, optical fiber link antenna measurement system, 6-axis vertically articulated robot with arm, antenna factor, friis transmission formular, amplitude center*

1. Introduction

The 5th generation mobile communication (5G) has already used the frequency band around 28 GHz [1]. Conventional antenna measurement usually uses a large anechoic chamber and some antenna measurement facilities such as a long coaxial cable, an antenna support mast, and a turn table. The use of metal coaxial cable for the 5G frequency band antenna measurement has some problems, such as signal attenuation in the cable (e.g., more than 3 dB per 1 m for the 28 GHz band), reflection waves on the outer surface, and handling difficulties. On the other hand, an optical fiber cable has some advantages for antenna measurements, such as signal attenuation in the cable (e.g., less than 0.2 dB per km for the 1550 nm wavelength), small reflection waves on the outer surface, and easy handling compared to coaxial cable. To reduce the disadvantage of the conventional antenna measurement system, we have developed an all-optical fiber link antenna measurement system that can replace the coaxial cables for the antenna measurement system.

We have developed an all-optical fiber link antenna measurement system, which consists of an optical fiber link electrical signal transmission system and a dual-polarized antenna-coupled electrode electric field (EO) sensor system as a electrical signal receiving system [2], [3]. The transmission system can transmit the electrical signal up to 40 GHz with more than −30 dBm output. In addition, for measuring the electric field intensity, we usually use an antenna factor of the EO sensor. We have already developed a far field antenna factor estimation method using the amplitude center modified antenna factor estimation equation [4], [5]. In the case of using the formula, we can estimate the far-field antenna factor of the antenna under test at the near distance. We have estimated the far-field antenna factor of the EO sensor using the formula [6].

In this paper, our developed the optical fiber link electrical signal transmission system and an antenna near-field measurement results for the system used for a standard gain horn antenna are first explained. Second, a dual-polarized antenna-coupled electrode electric field (EO) sensor system as a electrical signal receiving system is explained. Then, our developed all-optical fiber link antenna measurement system for the millimeter wave 5G frequency band around 28 GHz is explained. Then, we demonstrate an antenna radiation pattern measurement using the all-optical fiber link antenna measurement system. Finally, we show an antenna factor estimation equation using the amplitude center distance and the estimated far field antenna factor for the EO sensor system is explained.

2. All-Optical Fiber Link Antenna Measurement System Using an Industrial Robot System

2.1 Optical Fiber Link Electrical Signal Transmission System for Millimeter-Wave 5G Frequency Band [4]

We have already developed an optical fiber link electrical signal transmission system that consists of a zero bias optical reflection type electro-absorptive modulator (EAM) [7], a super luminescent diode (SLD: S5FC1005P of Thorlabs Inc. [8]), an optical circulator and a photodiode with transimpedance amplifier (PD-TIA: KPDX30G-T1 of Kyoto Semiconductor Co., Ltd.). Conventional EAM is usually driven by a DFB laser. To stabilize the time stability of the frequency response of the EAM, the conventional EAM

Manuscript received April 26, 2023.
Manuscript revised June 15, 2023.
Manuscript publicized September 19, 2023.

[†]The authors are with National Institute of Advanced Industrial Science and Technology (AIST), Tsukuba-shi, 305-8568 Japan.
[††]The authors are with Mie University, Tsu-shi, 514-8507 Japan.
[†††]The authors are with SEIKO GIKEN Co. Ltd., Matsudo-shi, 270-2214 Japan.
[††††]The author is with 7G aa Co. LTD., Tsukuba-shi, 305-0047 Japan.
a) E-mail: satoru-kurokawa@aist.go.jp
DOI: 10.1587/transcom.2023CEI0001

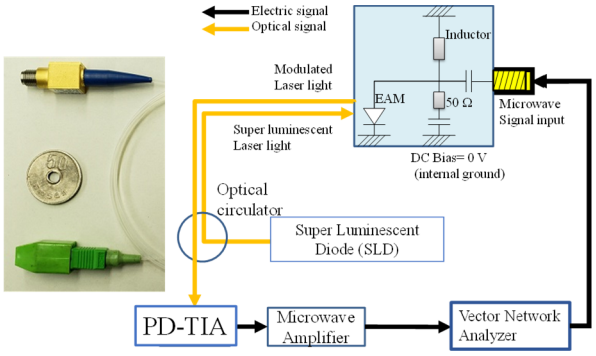

Fig. 1 Optical fiber link microwave transmission system.

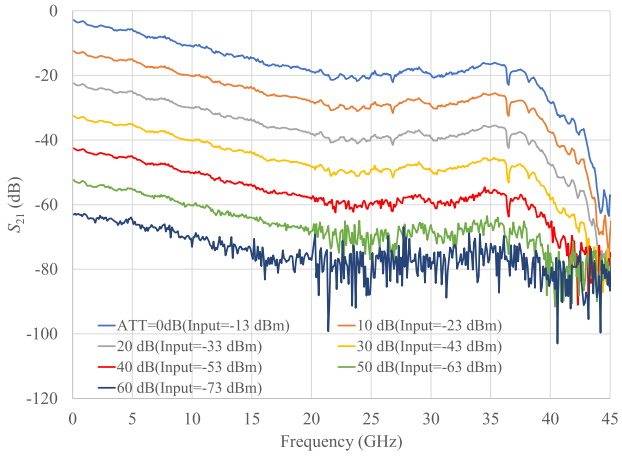

Fig. 2 Frequency characteristics of the optical fiber link microwave transmitting system.

usually uses a thermoelectric cooler (TEC) and DC bias. In the case of an EAM without TEC control, the frequency response and the DC bias point of the EAM fluctuate with the ambient temperature variation. In order to reduce the fluctuation of the frequency response of the EAM, we used the SLD as the input to the EAM. Figure 1 schematically shows the system with a vector network analyzer (VNA). The EAM connects to the port 1 of the VNA. The PD-TIA with an amplifier (GPA-280F, RF BAY Inc. [9]) connects to the port 2 of VNA. Figure 2 shows measured $S_{21}(\omega)$s of the system. Measured $S_{21}(\omega)$s of the system are more than −30 dB for the frequency range up to 40 GHz with more than 40 dB dynamic range.

In order to show the advantage of using the optical fiber link receiving system, we compared the antenna near field antenna measurement results between using the optical fiber link electrical signal transmission system with the EAM and using the coaxial cable system.

Figure 3 shows a photograph of a cylindrical antenna near field measurement setup using the optical fiber link electrical signal transmission system with an open-ended wave guide probe (OEWG) as the receiving antenna [10], [11]. The OEWG is mounted on the antenna support mast that can be moved from −1 m to +1 m from the center position for

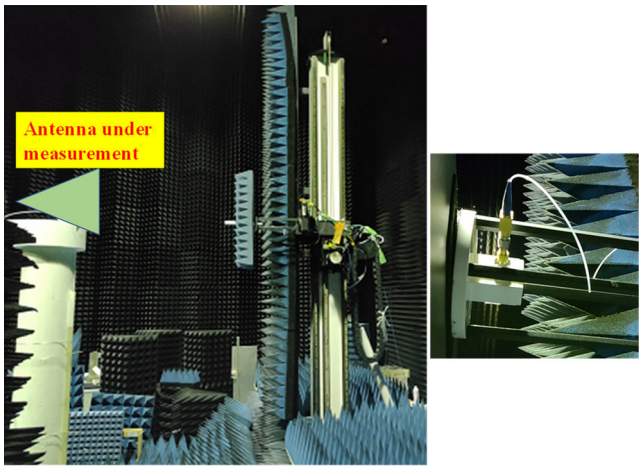

Fig. 3 Cylindrical antenna near field measurement setup using the optical fiber link transmission system with an open-ended wave guide probe.

the aperture of the antenna under test (AUT). The AUT is mounted on an azimuth turntable that can be moved from −180 degrees to +180 degrees. Figure 4 shows a measurement example for a cylindrical antenna near field measurement at 5.755 GHz for a standard gain horn antenna as the AUT, the azimuth angle from −40 degrees to +40 degrees, the OEWG position from −0.5 m to +0.5 m, comparing the use of the optical fiber link transmission system and the use of a coaxial cable system. The amplitude and phase measurement results of the coaxial cable system show fluctuations due to cable movement compared to the measurement results of the optical fiber link transmission system.

Figure 5 shows the difference of amplitude and phase, the azimuth angle from −40 degrees to +40 degrees, the OEWG position from −0.2 m to +0.3 m, between using the optical fiber link system and the coaxial cable system. The difference of the amplitude for these results are more than 1 dB. The difference of the phase for these results are more than 40 degrees. These results show that the optical fiber link transmission system can be used for near-field antenna measurements with less than 1 dB stability compared to the coaxial cable system at around 5.6 GHz.

2.2 Orthogonally Dual-Polarized Electric-Field Sensor as a Millimeter-Wave 5G Receiving Probe [3]

We have developed an optical fiber link receiving system using an antenna-coupled-electrode electric-field (EO) sensor system for the millimeter wave 5G frequency band around 30 GHz (EO no. 1) and 28 GHz (EO no. 2). The EO sensor is fabricated on a z cut $LiNbO_3$ film of about 50 μm thick that is stacked on a base substrate of SiO_2 glass about 250 μm thick. Two square patch antennas as receiving antennas are connected to a standing-wave resonant electrode by using microstrip feed lines to form an antenna-coupled electrode on the electric-field sensor. An optical waveguide as a phase modulator is fabricated on the reverse side of the $LiNbO_3$ film. The X-output port can receive the vertical polarization

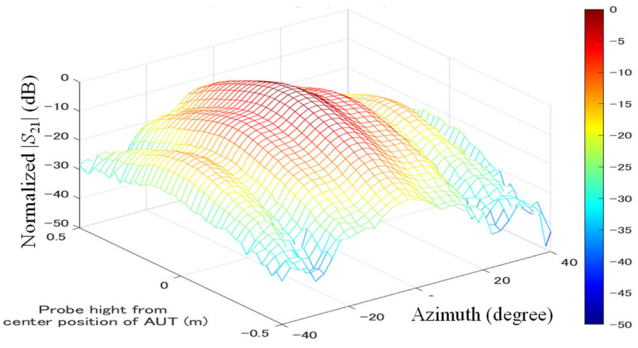

(a) Measured amplitude using the optical fiber link transmission system

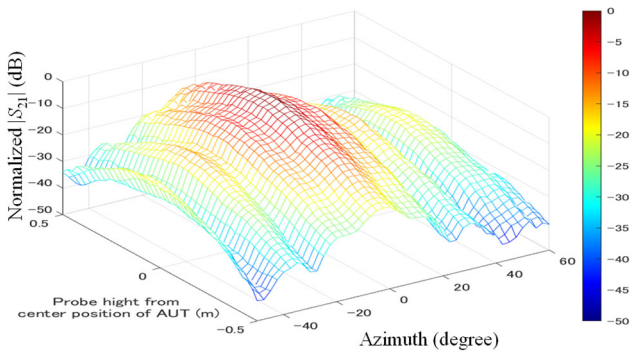

(b) Measured amplitude using the coaxial cable system

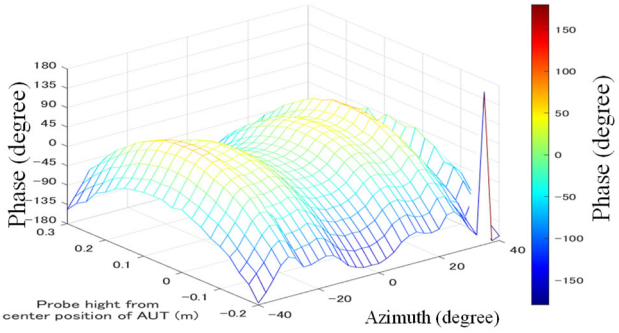

(c) Measured phase using the optical fiber link transmission system

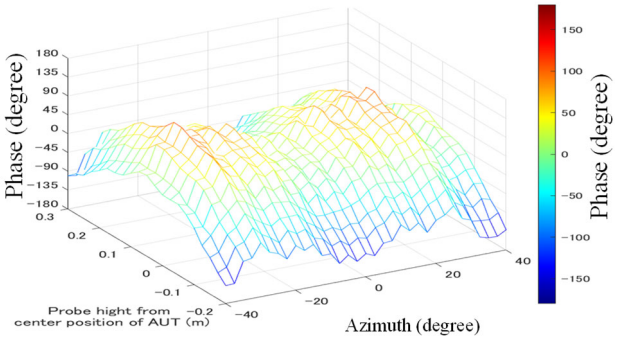

(d) Measured phase using the coaxial cable system

Fig. 4 Cylindrical antenna near field measurement result using the optical fiber link transmission system ((a) amplitude and (c) phase) and using the coaxial cable system ((b) amplitude and (d) phase).

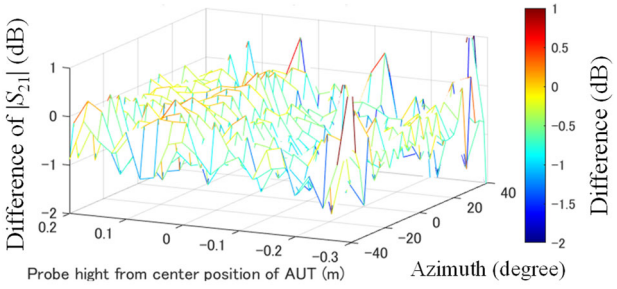

(a) Difference of S_{21} amplitude in dB

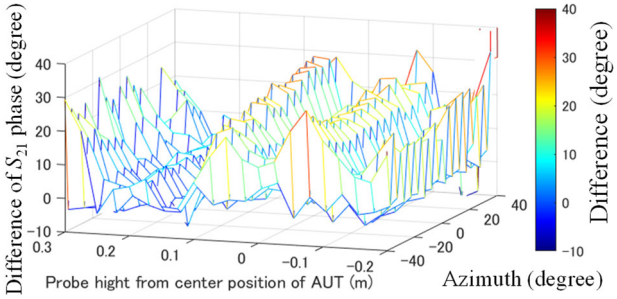

(b) Difference of S_{21} phase (degree)

Fig. 5 Difference of (a) amplitude and (b) phase between using the optical fiber link system and the coaxial cable system.

wave for the output port direction. The Y-output port can receive the horizontal polarization wave for the output port direction. Figure 6 shows an orthogonal dual-polarized EO sensor. The EO sensor is placed on an azimuth turntable to evaluate the receive pattern for the EO sensor. The standard gain horn antenna is mounted on the tip of the 6-axis Vertically Articulated Robot [12]. Figure 7 shows the measurement setup for the receiving pattern of the EO sensor using a 6-axis vertically articulated robot with an arm length of 1 m and the optical fiber link transmitting system. The frequency response of the EO no. 1 at the same polarization for the horn antenna and the cross polarization for the horn antenna are shown in Figs. 8 and 9, respectively. Figure 10 shows the estimated cross-polar discrimination ratio (XPD) for the EO no. 1 that is greater than 20 dB for the frequency range from 28 GHz to 28.9 GHz and 29.5 GHz to 31.5 GHz. These results show the fact that our developed EO sensor can simultaneously measure the same polarization electric field and cross-polarization electric field with XPD>15 dB for the frequency range from 28 GHz to 29 GHz and 30 GHz

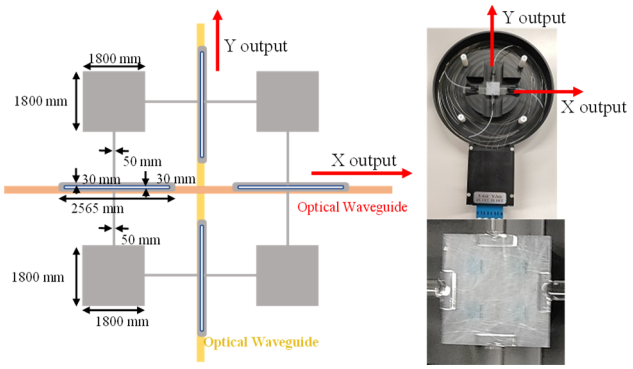

Fig. 6 Orthogonally dual-polarize type electric-field sensor.

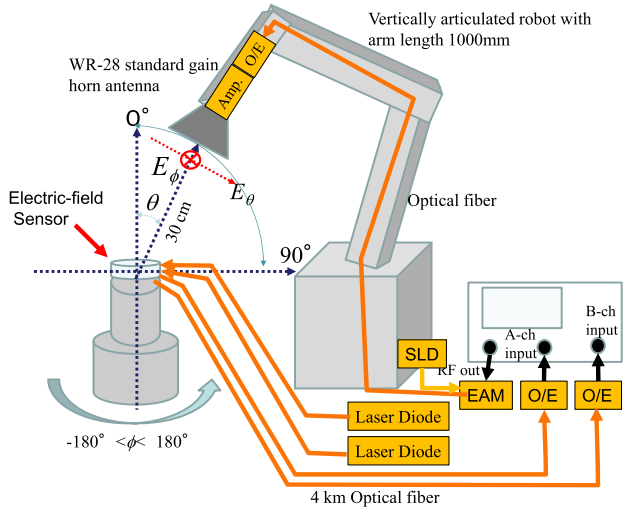

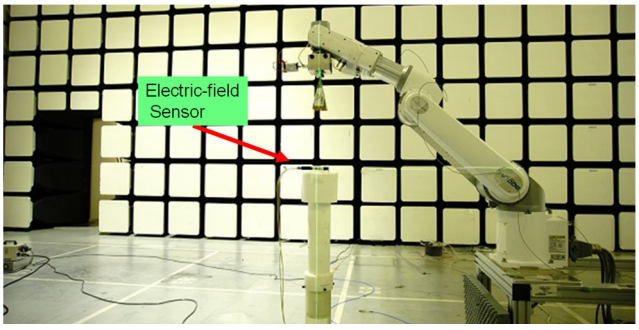

Fig. 7 Receiving pattern measurement setup for the EO sensor.

to 32 GHz.

The frequency response of the EO no. 2 at the same polarization for the horn antenna and the cross polarization for the horn antenna are shown in Figs. 11 and 12, respectively. Figure 13 shows the estimated cross-polar discrimination ratio (XPD) for the EO no. 2 that is greater than 15 dB for the frequency range from 27.5 GHz to 29.5 GHz. These results show the fact that our developed EO sensor can simultaneously measure the same polarization electric field and cross-polarization electric field with XPD>15 dB for the frequency range from 27.5 GHz to 29.5 GHz.

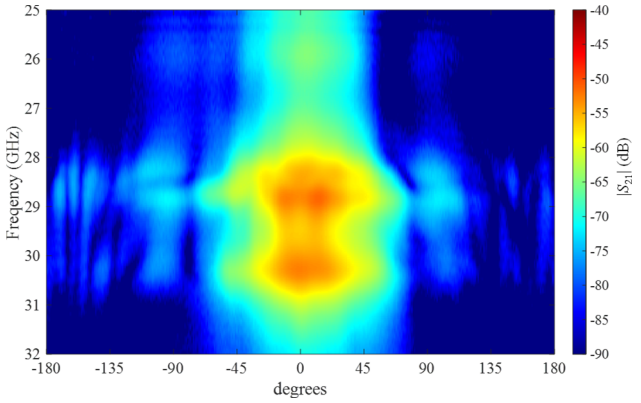

Fig. 8 E-plane receiving pattern for the EO sensor no. 1 (same polarization of the Horn antenna).

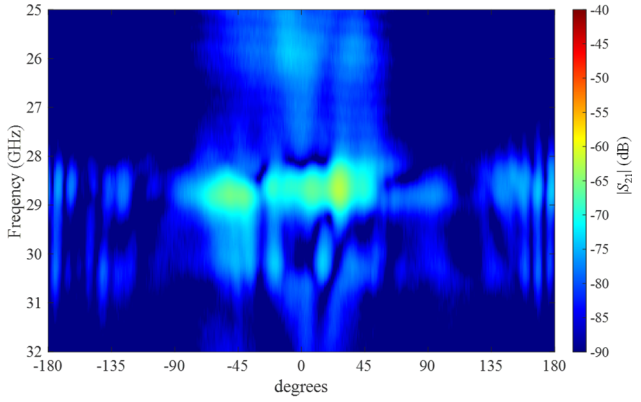

Fig. 9 E-plane receiving pattern for the EO sensor no. 1 (cross polarization of the Horn antenna).

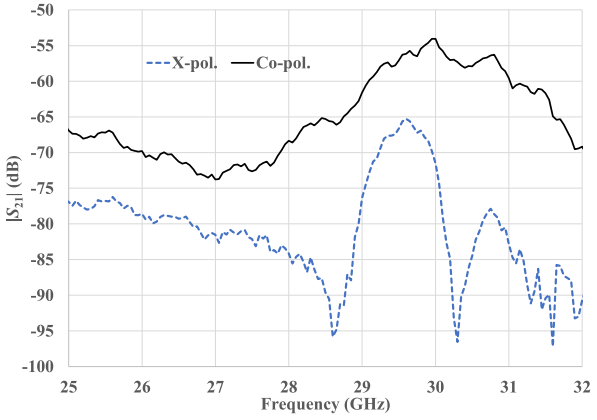

Fig. 10 Receiving level for the same polarization of the horn antenna (Co-pol.), the cross polarization of the horn antenna (X-pol.). (Receiving antenna is the EO sensor no. 1).

2.3 Antenna Pattern Measurement Using All Optical Fiber Link Antenna Measurement System Using the 6-Axis Vertical Articulated Robot [5]

We have demonstrated the H-plane radiation pattern mea-

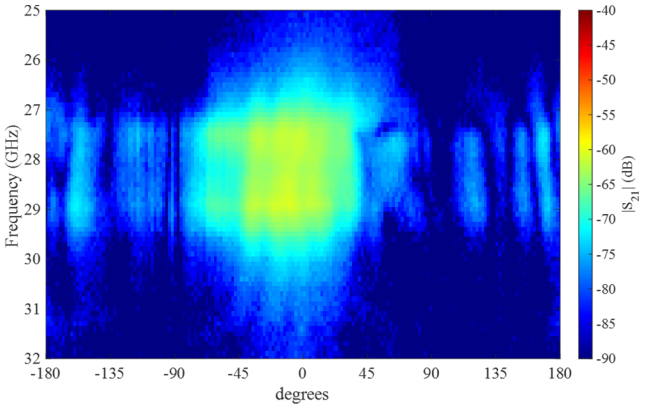

Fig. 11 E-plane receiving pattern for the EO sensor no. 2 (same polarization of the Horn antenna).

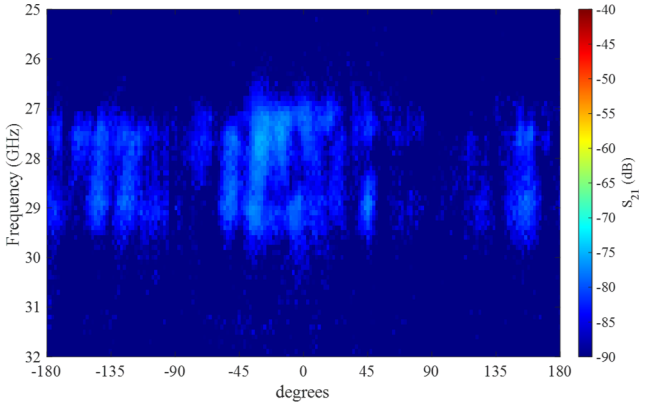

Fig. 12 E-plane receiving pattern for the EO sensor no. 2 (cross polarization of the Horn antenna).

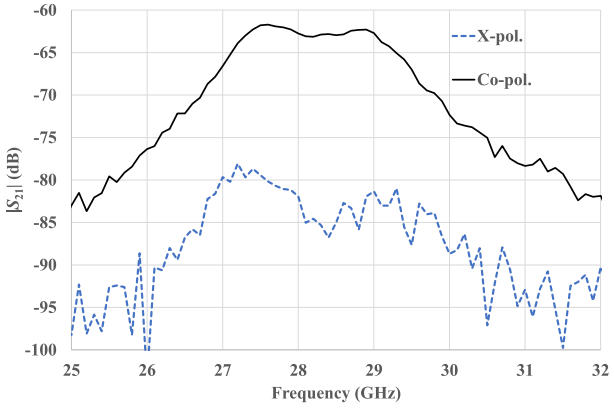

Fig. 13 Receiving level for the same polarization of the horn antenna (Co-pol.), the cross polarization of the horn antenna (X-pol.) and the difference between them (Difference). (Receiving antenna is the EO sensor no. 2).

surement for the WR-28 standard gain horn antenna as an AUT placed on an azimuth turntable. The EO sensor no. 1 is set to face to face for the aperture of the AUT with an antenna distance of 1 m between the aperture of the AUT and the aperture of the EO sensor. The EO sensor is mounted on the tip of the 6-axis vertically articulated robot. Our developed antenna pattern measurement system is shown in Fig. 14. The frequency characteristics of the $|S_{21}(\omega)|$ measured radiation pattern of the AUT depend on the frequency characteristics of the EO sensor in Fig. 15. Therefore, in Fig. 16, the measured $|S_{21}(\omega)|$s are normalized by the measured maximum $|S_{21}(\omega)|$s of each frequency. Figure 16 shows the fact that our developed EO sensor can measure the radiation pattern of the AUT with more than 45 dB dynamic range.

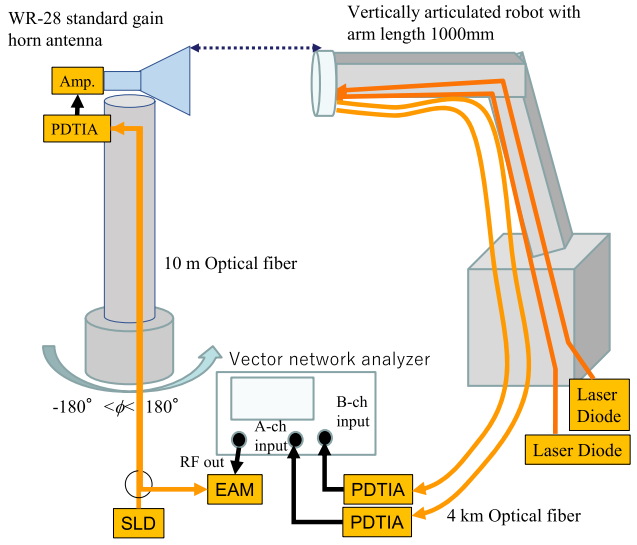

Fig. 14 Antenna radiation pattern measurement setup using all optical fiber link antenna measurement system using the industrial robot.

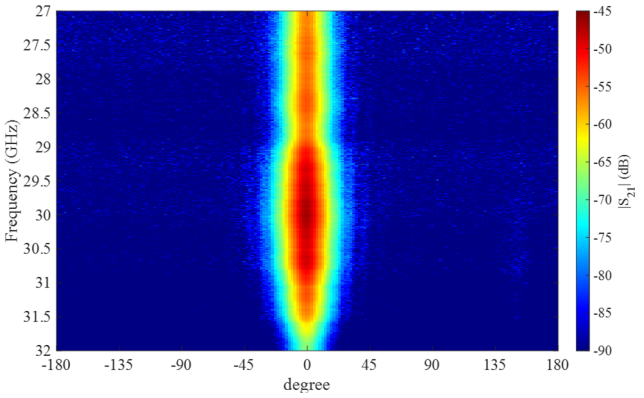

Fig. 15 Measured radiation pattern for the Horn antenna (same polarization for the EO sensor).

Figures 17 and 18 show the measured and the normalized (using the same polarization measurement results) radiation pattern for the cross-polarization of the EO sensor, respectively. The difference between the X-output level and the Y-output level (cross polar disclination ratio: XPD) is greater than 20 dB for the frequency range from 28 GHz to 29 GHz and 30 GHz to 32 GHz. These results show the fact that our developed all-optical antenna measurement system can measure the radiation pattern of the AUT for the frequency range from 28 GHz to 29 GHz and 30 GHz to 32 GHz with XPD>20 dB.

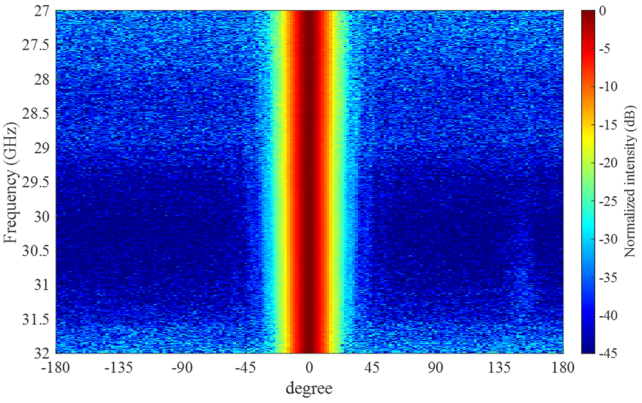

Fig. 16 Normalized measured radiation pattern for the Horn antenna (same polarization for the EO sensor).

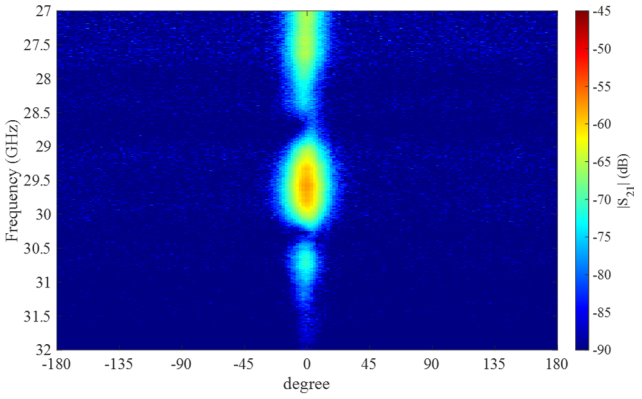

Fig. 17 Measured radiation pattern for the Horn antenna (cross polarization for the EO sensor no. 1).

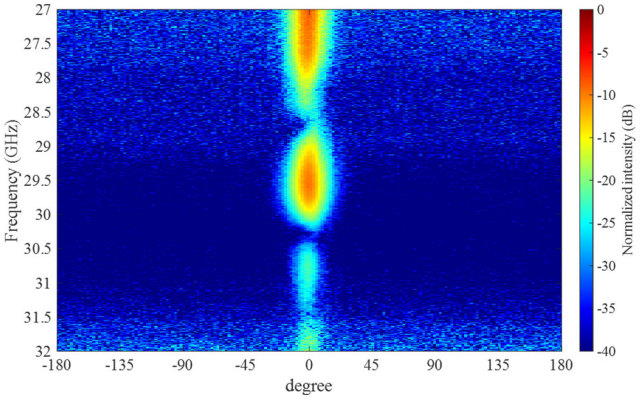

Fig. 18 Normalized measured radiation pattern for the Horn antenna (cross polarization for the EO sensor no. 1).

3. Antenna Factor Estimation for the Electric-Field Sensor Using an Amplitude Center Distance

3.1 Antenna Factor Estimation Equation Using the Amplitude Center Distance

In order to estimate the intensity of the electric field with the EO sensor, we use an antenna factor of the EO sensor. In order to estimate the far-field antenna factor at the near antenna distance, two antennas with the same polarization are placed face to face at the antenna distance = z. In this case, the frequency domain received signal $s_{21}(\omega, z)$ is shown in Eq. (1) [13] as

$$|s_{21}(\omega, z)| = \frac{\eta_0 \cdot k_0}{Z_0} \frac{1}{af_{\text{t\_NF}}(\omega, z)} \frac{1}{af_{\text{r\_NF}}(\omega, z)} \frac{1}{z} \tag{1}$$

where $af_{\text{t\_NF}}(\omega, z)$ and $af_{\text{r\_NF}}(\omega, z)$ are the near field antenna factors of the transmitting and receiving antennas, respectively. $\eta_0 = 120\,\pi\,\Omega$ is the intrinsic impedance of vacuum, $Z_0 = 50\,\Omega$ is the characteristic impedance of a vector network analyzer and the coaxial cable, and k_0 is the wave number in vacuum.

In the case of using amplitude center location, frequency domain receiving signal $s_{21}(\omega, z)$ is shown Eq. (2) [14]–[16] as

$$|s_{21}(\omega, z)| = \frac{\eta_0 \cdot k_0}{Z_0} \frac{1}{af_{\text{t\_far}}(\omega)} \frac{1}{af_{\text{r\_far}}(\omega)} \frac{1}{z + d_1(\omega) + d_2(\omega)} \tag{2}$$

where $af_{\text{t\_far}}(\omega)$ and $af_{\text{r\_far}}(\omega)$ are the far-field antenna factors of the transmitting and receiving antennas, respectively. $d_1(\omega)$ and $d_2(\omega)$ are the distances from the incident point to the amplitude center of the transmitting and receiving antennas, respectively. In the case of antenna distances between transmitting and receiving antennas are $z = z_1$ and z_2, measured frequency responses are $s_{21}(\omega, z_1)$ and $s_{21}(\omega, z_2)$, the far field antenna factors can be shown by the following equation,

$$af_{\text{t\_far}}(\omega) \cdot af_{\text{r\_far}}(\omega) = \frac{\eta_0 \cdot k_0}{Z_0} \left(\frac{1}{|s_{21}(\omega, z_1)|} - \frac{1}{|s_{21}(\omega, z_2)|} \right) \frac{1}{z_1 - z_2} \tag{3}$$

$$af_{\text{t\_far}}(\omega) \cdot af_{\text{r\_far}}(\omega) = \frac{\eta_0 \cdot k_0}{Z_0} A_{21} D_{21} \tag{4}$$

Where $A_{21} = \dfrac{1}{|s_{21}(\omega, z_1)|} - \dfrac{1}{|s_{21}(\omega, z_2)|}$, $D_{21} = \dfrac{1}{z_1 - z_2}$

3.2 Measurement Setup for the Antenna Factor Measurement of the EO Sensor

In the case of using the calibrated antenna factor for the transmitting antenna $af_{\text{t\_far}}(\omega)$, we can estimate the far field antenna factor for the receiving antenna $af_{\text{r\_far}}(\omega)$ using the Eq. (4). To determine the antenna distance for the far field antenna factor of the EO sensor no. 2, we have measured the $S_{21}(\omega, z)$s for the antenna distance between the aperture of the WR-28 standard gain horn antenna (far field distance < 1.0 m) as the transmitting antenna and the EO sensor from $z = 1.0$ m to 2.9 m every 0.1 m. Figure 19 shows the antenna factor measurement setup. Figure 20 shows measured $S_{21}(\omega, z)$s after removing the ambient reflection waves by using the time domain estimation. Then, we estimated the

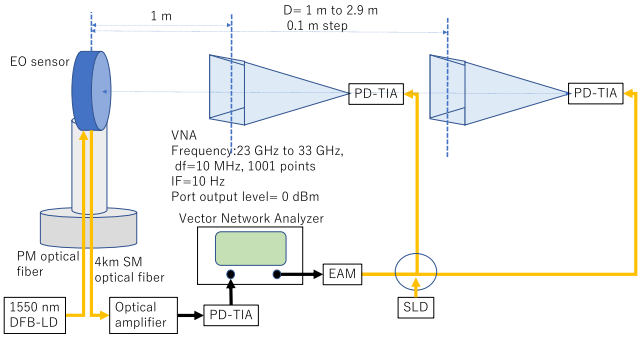

Fig. 19 Antenna factor measurement setup for the EO sensor using the WR-28 standard gain horn antenna as a transmission antenna.

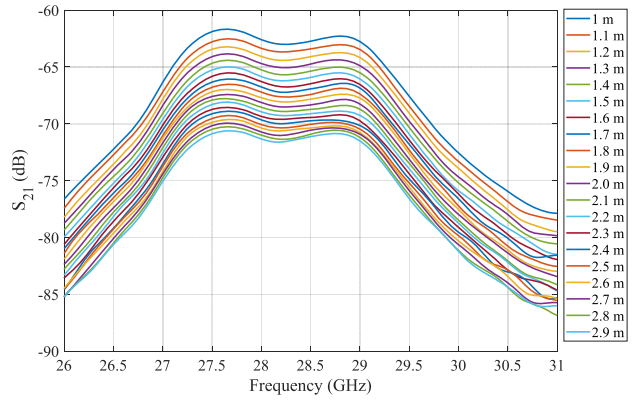

Fig. 20 Measured $S_{21}(\omega, z)$s after removing the ambient reflection waves.

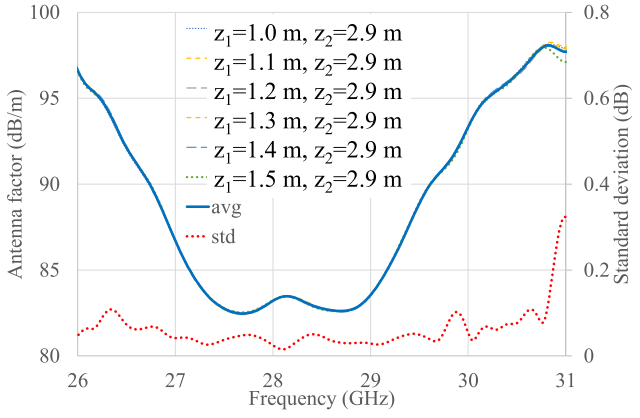

Fig. 21 Estimated far field antenna factors of the EO sensor no. 2 using the Eq. (4) for the measured $S_{21}(\omega, z_1)$s of z_1 = 1.0 m, 1.1 m, 1.2 m, 1.3 m, 1.4 m, 1.5 m and $S_{21}(\omega, z_2)$s of z_2 = 2.9 m, the average of these antenna factors (blue line), and standard deviation of these antenna factors (red dotted line).

antenna factors using the $S_{21}(\omega, z_2)$s with z_2 = 2.9 m and each of the $S_{21}(\omega, z_1)$s with z_1 = 1.0 m, 1.1 m, 1.2 m, 1.3 m, 1.4 m, 1.5 m using the Eq. (4). Figure 21 shows the estimated antenna factors, the average of these antenna factors, and the standard deviation of these antenna factors. These results show that the standard deviation of the measured antenna factors of the EO sensor no. 2 is less than 0.1 dB the measured antenna factor is 83.2 dB/m at 28 GHz. These results show the fact that the EO sensor can measure the electric field using the estimated antenna factor of the EO sensor system around 28 GHz band.

4. Conclusions

We have developed an all-optical fiber link antenna measurement system for the millimeter wave 5th generation mobile communication (5G) frequency band around 28 GHz. For the millimeter-wave 5G measurement, we developed an electrical signal transmission system consisting of the optical reflection type EA modulator and PD-TIA as for the antenna near field measurement. In addition, we have developed the orthogonally polarized simultaneous receiving EO sensor that can measure the electric field around 28 GHz and 30 GHz. We have shown the measurement results for the WR-28 standard gain horn antenna.

In addition, we show the method of estimating the far antenna factor for the EO sensor. The estimated standard deviation of the measured antenna factors of EO sensor no. 2 is less than 0.1 dB, and the measured antenna factor is 83.2 dB/m at 28 GHz. These results show the fact that the EO sensor can measure the electric field using the estimated antenna factor of the EO sensor system around 28 GHz band.

The beyond 5G and 6G mobile communication services will use the frequency band above 60 GHz, D band (110 GHz to 170 GHz) and J band (220 GHz to 300 GHz). In this case, antenna measurement requires the optical fiber link electrical signal transmission system for the beyond 5G and 6G frequency band. In the future, we plan to develop an EO sensor for the beyond 5G and 6G frequency band.

Acknowledgments

The authors would like to thank Emeritus Professor Ishizone of Toyo University for helpful discussions on the measurements.

References

[1] Leading towards Next Generation “5G” Mobile Services. Federal Communications Commission. https://www.fcc.gov/news-events/blog/2015/08/03/leading-towards-next-generation-5g-mobile-services
[2] H. Murata, H. Yokohashi, S. Matsukawa, M. Sato, M. Onizawa, and S. Kurokawa, “Antenna-coupled electrode electro-optic modulator for 5G mobile applications,” IEEE J. Microw., vol.1, no.4, pp.902–907, Oct. 2021.
[3] S. Nakamori, H. Yokohashi, Y. Otagaki, S. Matsukawa, M. Sato, M. Onizawa, S. Kurokawa, and H. Murata, “Antenna-coupled-electrode electro-optic modulator for converting 5G-band wireless signal with two orthogonal-polarization field components,” Proc. OECC/PSC 2022, July 2022.
[4] S. Kurokawa and M. Hirose, “Far field antenna factor estimation method by the subtraction of unwanted waves using pulse compression and time-domain technique,” IEICE Trans. Commun. (Japanese Edition), vol.J101-B, no.9, pp.660–674, Sept. 2018.
[5] S. Kurokawa, M. Ameya, S. Matsukawa, M. Sato, M. Onizawa, H. Murata, and M. Hirose, “All-optical fiber link antenna measurement system using an industrial robot system,” Proc. EuCAP2022, March

2022.
[6] S. Kurokawa, S. Matsukawa, M. Ameya, M. Sato, M. Onizawa, and H. Murata, "Antenna factor estimation for electric-field sensor using an amplitude center modified Friis transmission formular," Proc. 2021 IEEE CAMA, Nov. 2021.
[7] S. Kurokawa, M. Ameya, and M. Hirose, "A novel evaluation method for semi-anechoic chamber using zero biased optical devices and time-domain analysis," Proc. ICWITS 2010, Aug. 2010.
[8] PM benchtop SLD Source S5FC1005P, 1550 nm, 22 mW, 50 nm Bandwidth, https://www.thorlabs.com/thorproduct.cfm?partnumber=S5FC1005P
[9] RF Amplifier GPA-280F, 20 GHz–36 GHz, RF BAY, Inc., https://rfbayinc.com/products_pdf/product_433.pdf
[10] IEEE Std 1720-2012, IEEE Recommended Practice for Near-Field Antenna Measurements, 2012.
[11] L.J. Foged, J. Dobbins, V. Rodriguez, J. Fordham, and V. Monebhurrun, "Revision of IEEE Std. 1720-2012: Recommended practice for near-field antenna measurements," Proc. 2022 IEEE AP-S/URSI, pp.663–664, July 2022.
[12] Vertical Articulated Robot TV1000, Shibaura Machine Co., LTD., https://www.shibaura-machine.co.jp/en/product/robot/lineup/tv/tv1000.html
[13] S. Kurokawa, M. Hirose, and K. Komiyama, "Measurement and uncertainty analysis of free-space antenna factors of a log-periodic antenna using time-domain techniques," IEEE Trans. Instrum. Meas., vol.58, no.4, pp.1120–1125, April 2009.
[14] S. Kurokawa, M. Ameya, and M. Hirose, "Far filed gain estimation method for Japanese broadband antenna standard using time-frequency analysis," Proc. PIERS 2013, Stockholm, Sweden, pp.838–842, Aug. 2013.
[15] S. Kurokawa, M. Hirose, and M. Ameya, "Far field antenna factor estimation method for super broadband antenna using time-frequency analysis," Proc. IEEE CPEM 2014, July 2014.
[16] S. Kurokawa and M. Hirose, "Measurement uncertainty of free space antenna factor for super broadband antenna using amplitude center modified equation," Proc. IEEE CPEM 2016, July 2016.

Satoru Kurokawa received the B.E. and M.E. degrees in electrical engineering from Chiba University, Chiba, Japan, in 1987 and 1989, respectively, and the Ph.D. degree from the Department of Communication and Computer Engineering, Kyoto University, Kyoto, Japan, in 2002. Since 2003, he was a senior researcher at the National Metrology Institute of Japan (NMIJ), National Institute of Advanced Industrial Science and Technology (AIST), Ibaraki, Japan. Since 2022, he has been the manager of the International Cooperation Office of NMIJ, AIST. His research interests include antenna metrology, radio over fiber technology for antenna measurement, electromagnetic interference measurement, and time-domain measurement. He is the Technical Adviser of 7G aa Company, Ltd. He was the General Co-Chair of the 2017 IEEE Conference on Antenna Measurements and Applications (2017 IEEE CAMA). He is an Advisory Committee Member of the IEICE Photonic Applied Electromagnetic Measurement Technical Committee. From 2019 to 2022, he was the Vice-Chair of the IEICE Antennas and Propagation Technical Committee. He has been an International Secretary of IEC TC103. He has been the Japan Node Chair of AMTA (Antenna Measurement Techniques Association) since October 2023.

Michitaka Ameya received the B.E. and M.E. degrees from the Department of Electronic Engineering, Hokkaido University, Hokkaido, Japan, and the Ph.D. degree from the Graduate School of Information Science and Technology, Hokkaido University, in 2003, 2005, and 2008, respectively. He has been a Senior Researcher with the National Metrology Institute of Japan, National Institute of Advanced Industrial Science and Technology, Tsukuba, Japan, since 2008. His current research interests include electromagnetic compatibility, millimeter-wave antenna calibration, and 5G array antenna testing by machine learning algorithm.

Yui Otagaki received the B.E. and M.E. degrees from the Department of Electronic Engineering, Osaka University, Osaka, Japan.

Hiroshi Murata was born in Osaka, Japan, in October 1965. He received the B.Eng., M.Eng., and D.Eng. degrees in electrical engineering from Osaka University, Osaka, Japan, in 1988, 1990, and 1998, respectively, for studies on the nonlinear optical waveguides and their applications to all-optical functional devices. In 1991, he joined the Department of Electrical Engineering, Faculty of Engineering Science, Osaka University. In 2018, he moved to the Area of Electric and Electronic Engineering, Graduate School of Engineering, Mie University, Tsu, Japan, where he is currently a Professor. He is the author or coauthor of more than 260 scientific publications in his areas of research, and also holds various patents. His research interests include 5G/Beyond 5G mobile systems, microwave photonics, integrated optics, and nonlinear optics. He was an Associate Editor for IEICE Electronics Express (ELEX) in Japan, in 2009–2012 and was the Guest Editor of the Special Issue on Progress in Domain-Engineered Photonic Materials in the Journal Advances in Opto-Electronics, in 2007–2008. He is also a member of the IEEE Photonics and MTT societies, OSA, EuMA, JSAP, IEICE, the Laser Society of Japan, the Optical Society of Japan, and the Institute of Image Information and Television Engineers of Japan. He was the recipient of the 35th European Microwave Conference Microwave Prize in 2005, the IEEE Photonics Global Singapore Best Paper Award in 2008, the 2017 Micro-Optics Conference Paper Award in 2017, and the IEC 1906 Award in 2017.

Masatoshi Onizawa received the B.E. degree in electronic engineering from The University of Electro-Communications, Tokyo, Japan, in 2000. In 2000, he joined TOKIN Corporation, Shiroishi, Japan, where he was in the development of optical communication equipment for broadcasting. In 2006, he moved to SEIKOH GIKEN Company Ltd., Japan. He is currently engaged in radio-over fiber equipment development and manufacturing.

Masahiro Sato received the B.E. degree in polymer material engineering from Yamagata University, Yamagata, Japan, in 1989. In 1989, he joined TOKIN Corporation, Shiroishi, Japan, where he was in the development of semiconductor application devices. In 2006, he moved to SEIKOH GIKEN Company Ltd. He is currently engaged in optical device development and manufacturing.

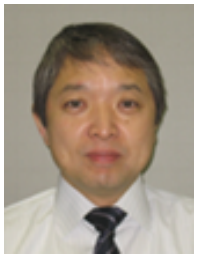

Masanobu Hirose received the B.E. degree in physics from Kanazawa University, Kanazawa, Japan, in 1979, the M.S. degree in physics from Hiroshima University, Hiroshima, Japan, in 1981, and the M.E. and D.E. degrees in electrical engineering from the University of Electro-Communications, Tokyo, Japan, in 1983 and 1999 respectively. From 2000 to 2019, he was a Senior Researcher with the Metrology Institute of Japan, National Institute of Advanced Industrial Science and Technology, Tsukuba, Japan. Since 2020, he has been the CEO of 7G aa Company, Ltd., Tsukuba, Japan. His current research interests include near-field antenna measurements and computational electromagnetics.